J|A|C|S
ARTICLES
Published on Web 11/23/2002

Functional Specificities of Methylglyoxal Synthase and Triosephosphate Isomerase: A Combined QM/MM Analysis

Xiaodong Zhang,[†] David H. T. Harrison,[‡] and Qiang Cui*,[†]

Contribution from the Department of Chemistry and Theoretical Chemistry Institute, University of Wisconsin—Madison, 1101 University Avenue, Madison, Wisconsin 53706, and Department of Biochemistry, Medical College of Wisconsin, 8701 Watertown Plank Road, Milwaukee, Wisconsin 53226

Received May 27, 2002

Abstract: Combined SCC-DFTB/CHARMM calculations were carried out to analyze the origin for the functional specificities of triosephosphate isomerase (TIM) and methylglyoxal synthase (MGS). The two enzymes bind to the same substrate, dihydroxyacetone phosphate (DHAP), and have rather similar active sites. However, they catalyze different reactions; TIM catalyzes the isomerization of DHAP to glyceraldehyde 3-phosphate (GAP), while MGS catalyzes the elimination of phosphate from DHAP. Similar to previous suggestions, the calculations confirmed that GAP formation is prohibited in MGS due primarily to the reduced flexibility of the catalytic base (Asp 71) compared to that in TIM (Glu 165). For the suppression of phosphate elimination in TIM, the calculations show that the widely accepted stereoelectronic argument that invokes the different phosphoryl torsion angles observed in the X-ray structures of inhibitor complexes of the two enzymes is not as important as electrostatic contributions from the protein and water molecules surrounding the phosphoryl.

I. Introduction

Enzymes are fascinating and overshadow most chemical catalysts because they are not only efficient but also highly reaction *specific*; i.e., they are constructed by evolution such that the amount of byproduct is minimized.[1] Investigations of enzyme catalysis should address, therefore, both the issues of efficiency and specificity. In this regard, it is striking that very few theoretical studies have investigated specificity and most previous calculations have focused merely on the catalytic efficiency.[2,3] In this work, we use theoretical methods to explore the origin of the catalytic specificities of methylglyoxal synthase (MGS) and triosephosphate isomerase (TIM). It is shown that, in contrast to the stereolelectronic hypothesis[4] that has been widely accepted, the functional specificities of the two enzymes are due mainly to the difference in the electrostatic environment of the substrate binding pocket. The current study highlights the power of combining theoretical approaches and X-ray structures to go beyond the "static" views provided by the latter when interpreting enzyme catalytic mechanisms.

MGS is an enzyme that catalyzes the first reaction in the methylglyoxal bypass of the Embden—Myerhoff glycolytic pathway;[5] the methylglyoxal metabolism is of biomedical interest because methylglyoxal is implicated in diabetic complications.[6] MGS shares neither sequence nor overall structural[7−9] similarity with TIM, yet both enzymes bind dihydroxyacetone phosphate (DHAP) as the natural substrate. The reactions that the two enzymes catalyze, however, are rather different (Scheme 1). While TIM catalyzes the isomerization between DHAP and GAP ((*R*)-glyceraldehyde 3-phosphate) *bidirectionally*,[10] MGS catalyzes the elimination reaction of DHAP, which leads to inorganic phosphate and the enol of methylglyoxal (subsequently tautomerizes to methylglyoxal in solution), and does *not* catalyze the elimination reaction with GAP as the substrate.[9,11] The elimination reaction of enediolate phosphates in solution is faster than isomerization by at least a factor of 100,[12] while the former is suppressed by a factor of 10^{5-8} in TIM.[13] The specificities of the two enzymes are more impressive in light of the striking similarity in their active sites (Figure 1); both have a base (Glu 165 in TIM and Asp 71 in MGS[14]), a histidine (His 95 in TIM and His 98 in MGS), and a lysine (Lys 12 in TIM and Lys 23 in MGS) close to the substrate. Both MGS and TIM catalyze their set of reactions near the diffusion limit with similar kinetics.[9,10] Therefore, MGS and TIM form a remarkable pair of examples for catalytic *efficiency* and *specificity*.

* Corresponding author. E-mail: cui@chem.wisc.edu.
[†] University of Wisconsin—Madison.
[‡] Medical College of Wisconsin.

(1) See, for example: Fersht, A. *Structure and mechanism in protein science*; W. H. Freeman: New York, 2001.
(2) Bruice, T. C.; Kahn, K. *Curr. Opinion Struct. Biol*. **2000**, *4*, 540.
(3) See, for example, Field, M. J. *J. Comput. Chem.* **2002**, *23*, 48.
(4) (a) Deslongchamps, P.; Atlani, P.; Frehel, D.; Malaval, A. *Can. J. Chem*. **1972**, *50*, 3405. (b) Kirby, A. J. *The Anomeric Effect and Related Stereoelectronic Effects at Oxygen*, Springer-Verlag: Berlin, 1983.
(5) Cooper, R. A. *Annu. Rev. Microbiol*. **1984**, *44*, 812.
(6) Brownlee, M.; Cerami, A. *Annu. Rev. Biochem*. **1981**, *50*, 385.
(7) Davenport, R. C.; Bash, P. A.; Seaton, B. A.; Karplus, M.; Petsko, G. A.; Ringe, D. *Biochemistry* **1990**, *30*, 5821.
(8) Saadat, D.; Harrison, D. H. T. *Biochemistry* **2000**, *39*, 2950.
(9) For a recent discussion, see, Marks, G. T.; Harris, T. K.; Massiah, M. A.; Mildvan, A. S.; Harrison, D. H. T. *Biochemistry* **2001**, *40*, 6805.
(10) Knowles, J. R.; Albery, W. J. *Acc. Chem. Res*. **1977**, *10*, 105.
(11) Tsai, P.; Gracy, R. W. *J. Biol. Chem.* **1976**, *251*, 365.
(12) Richard, J. P. *J. Am. Chem. Soc*. **1984**, *106*, 4926.
(13) Richard, J. P. *Biochemistry* **1991**, *30*, 4581.
(14) Saadat, D.; Harrison, D. H. T. *Biochemistry* **1998**, *37*, 10074.

10.1021/ja027063x CCC: $22.00

Scheme 1

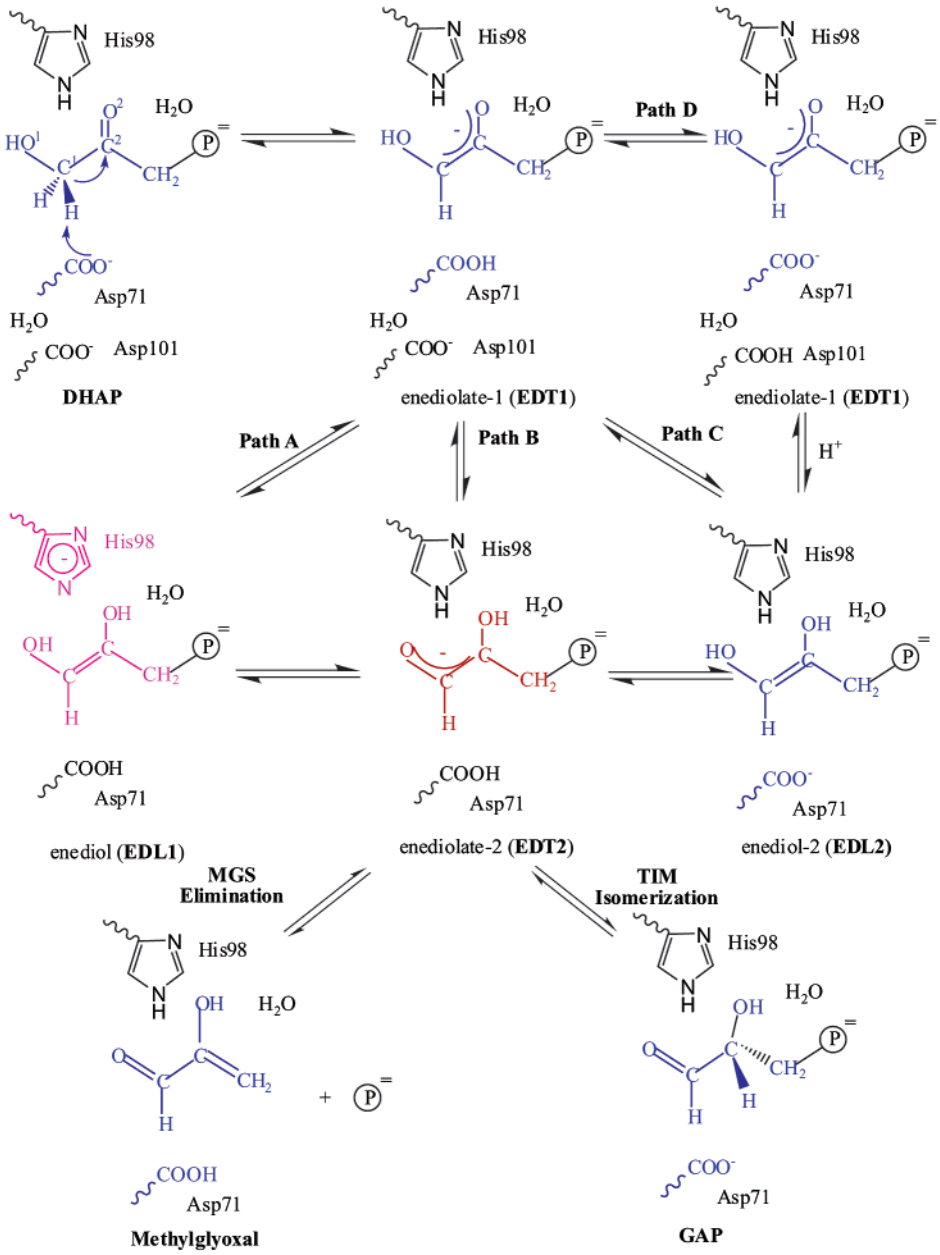

Although much is known about the catalytic mechanism of TIM following extensive experimental[15] and theoretical efforts,[16,17] the detailed catalytic mechanism of MGS and factors that control the catalytic specificities of TIM and MGS are less established. For example, there are several possible proton transfer pathways for the initial part of the MGS catalysis, one of which was only recently proposed based on mutation, inhibition, and structural studies.[9] These proton-transfer pathways in MGS have been analyzed and compared to TIM computationally.[18] It was found that the "classical" TIM mechanism (path A shown in Scheme 1) is also energetically reasonable in MGS and will be used for the purpose of this paper; detailed results will be published separately.[18] Related to the specificity issue, two structural features observed from the PGH·MGS[9] (PGH: phosphoglycolohydroxamate) and PGH·TIM[7] X-ray data have been noticed previously. First, the general acid for GAP formation in MGS is an aspartic acid (Asp 71), which is less flexible than the glutamic acid (Glu 165) in TIM; this has been related to the fact that GAP formation is much less favored in MGS than in TIM.[9] On the different propensities toward phosphate elimination, the traditional hypothesis is based on a stereoelectronic argument.[4] It was found that the $O^2-C^2-C^3-O^3$ torsional angle (Figure 1) of the competitive inhibitor is quite different in the two enzymes; it is ~45° in MGS and ~15° in TIM for PGH, and ~55° in MGS and ~5° in TIM for PGA (phosphoglycolate). Therefore, the orbital overlaps between the breaking C^3-O^3 bond and the enediol π system could be very different in the two enzymes, which would make the

(15) For a recent review, see: Knowles, J. R. *Nature* **1991**, *350*, 121.
(16) (a) Cui, Q.; Karplus, M. *J. Am. Chem. Soc.* **2001**, *122*, 2284. (b) Cui, Q.; Karplus, M. *J. Phys. Chem. B* **2002**, *106*, 1768. (c) Cui, Q.; Karplus, M. *J. Am. Chem. Soc.* **2002**, *124*, 3093.
(17) (a) Bash, P. A.; Field, M. J.; Davenport, R. C.; Petsko, G. A.; Ringe, D.; Karplus, M. *Biochem.* **1991**, *30*, 5826. (b) Alagona, G.; Ghio, C.; Kollman, P. A. *J. Am. Chem. Soc.* **1995**, *117*, 9855. (c) Åqvist, J.; Fothergill, M. *J. Biol. Chem.* **1996**, *271*, 10010.
(18) Zhang, X.; Harris, D. H. T.; Cui, Q. Unpublished.

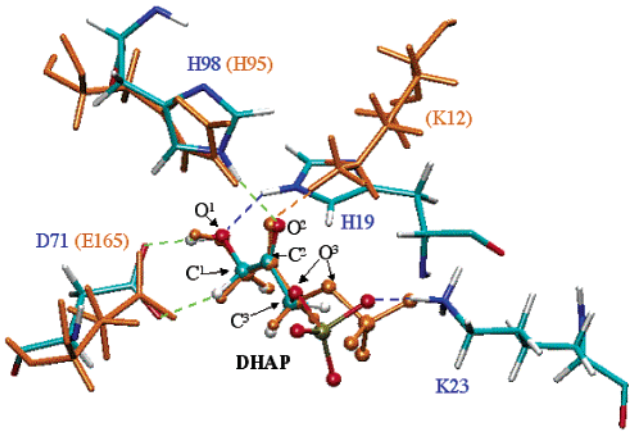

Figure 1. A comparison of active site arrangements in methylglyoxal synthase (MGS) and triosephosphate isomerase (TIM) based on the X-ray structures with PGH as the substrate analogue (replaced by DHAP in the figure). The substrate is shown in ball-and-stick, and protein residues are shown in line forms; the MGS residues are colored according to atom types, and those in TIM are shown in orange. The hydrogen-bonding interactions found in both enzymes are shown in green; those found specifically in MGS and TIM are shown in blue and orange, respectively. Note the similarity in the orientations of the catalytic base (Asp 71 in MGS and Glu 165 in TIM) and the distal histidine (H98 in MGS and H95 in TIM) relative to the substrate. The phosphate torsional angle ($O^2-C^2-C^3-O^3$) is rather different in the two enzymes. Also note that there is a Lys residue close to the substrate in both enzymes (Lys 23 in MGS and Lys 12 in TIM), although the position of this Lys relative to the phosphate is quite different; such a difference is proposed to be essential to the functional specificity of MGS (see the text). The figure was prepared with VMD (Humphrey, W.; Dalke, A.; Schulten, K. *J. Mol. Graph.* **1996**, 14, 33).

elimination reaction less favorable in TIM than in MGS.[19] Although those arguments are physically reasonable, no quantitative measurement is available, and other structural and electrostatic effects might make substantial contributions to the specificities. For example, while there are only two hydrogen bonds from adjacent residues that stabilize the phosphate in TIM, there are about 11 in MGS; the water structure around the phosphate is also very different in the two enzymes.[8,9] To clarify the origin for the functional specificities of MGS vs TIM, we carried out theoretical analysis for the energetics of the isomerization and phosphate elimination reactions in the two enzymes using a combined QM/MM approach[20] with SCC-DFTB[21] as the QM method. The setup of the computations is described in section II, the results and analysis are presented in section III, and several conclusions are summarized in section IV.

II. Computational Methods

The current simulation was set up with the stochastic boundary condition[22] similar to previous studies of triosephosphate isomerase.[16] As the starting structure, the 1.8 Å resolution X-ray structure of the MGS−PGH complex (PDB code 1IK4) was used with the HNOH group of PGH replaced by H_2COH of DHAP; the rms difference from the X-ray structure of the heavy atoms in the active region of the stochastic boundary system was 0.35 Å (0.50 Å) for the main chain (all heavy atoms) after minimization. A stochastic boundary treatment[22] of the active site in one of the subunits of radius 25 Å (some residues, particularly Arg 107 and 150, of another subunit were included and contribute to the catalysis) was used, and the final model included 4136 protein atoms and 1114 water molecules. A Poisson−Boltzmann (PB) charge-scaling scheme[23] was introduced to account for solvent shielding in addition to that from the explicit water molecules in the model. The algorithm makes use of several PB calculations to determine a set of scaling factors to reduce the partial charges of charged side chains in the QM/MM calculations so as to avoid artifactual structural changes.[16] After the simulations are completed, another set of PB calculations can be carried out to correct for the charge scaling and include solvation effects for the fully charged system.[23]

The QM region in the QM/MM calculations included the substrate, Asp 71, His 19, His 98, and Wat 30; Lys 23 was also included in selected calculations. Link atoms were introduced to saturate the valence of the QM boundary atoms; the link atoms interact with the MM atoms, except the "link host" MM atom (e.g., the Cα atoms in this case), through electrostatic terms; no van der Waals interactions are included. This scheme has been shown to be a satisfactory way to treat the QM/MM interface, particularly when the charges of the atom in the neighborhood of the link atom are small;[24] this is true in the present case. The self-consistent-charge density functional tight binding (SCC-DFTB)[21] approach, which was introduced into CHARMM[25] recently in a combined QM/MM framework,[34] was used as the QM method. SCC-DFTB is an approximate density functional method, and extensive tests for hydrogen-bonding systems[26] and proton/hydride transfer reactions[34,27] indicate that it is more accurate than the standard semiempirical methods such as AM1 and PM3 with a similar computational speed. For example, SCC-DFTB/MM has been shown to give satisfactory results for TIM compared to B3LYP[28]/6-31+G-(d,p)[29]/CHARMM calculations (ref 34); test calculations also indicate that it describes the elimination reaction of phosphate well in model systems (see Supporting Information). The set of van der Waals parameters optimized in previous studies for TIM were used for the QM atoms;[16,34] QM/MM calculations with this set of parameters gave reliable results for model systems compared to full QM calculations.[16,34]

To determine the energtics for proton-transfer steps (see path A in Scheme 1), the adiabatic mapping calculations were carried out using the antisymmetric stretch involving the proton donor, the transferring proton, and the proton acceptor as the reaction coordinate. Such an approach was found to be sufficient for analyzing barrier heights associated with proton-transfer reactions in previous studies of triose-phosphate isomerase,[16] based on comparisons with more rigorous saddle point optimizations[16b] and potential of mean force calculations.[16c] The results are also in good agreement with preliminary potential of mean

(19) (a) Lolis, E.; Petsko, G. A. *Biochemistry* **1990**, *29*, 6619. (b) Pompliano, D. L.; Peyman, A.; Knowles, J. R. *Biochemistry* **1990**, *29*, 3186.
(20) (a) Field, M.; Bash, P. A.; Karplus, M. *J. Comput. Chem*. **1990**, *11*, 700. (b) Gao, J. In *Reviews in Computational Chemistry*; Lipkowitza, K. B, Boyd, D. B., Eds.; VCH: New York, 1996; Vol. 7, p 119. (c) Åqvist, J.; Warshel, A. *Chem. Rev*. **1993**, 93, 2523.
(21) Elstner, M.; Porezag, D.; Jungnickel, G.; Elsner, J.; Haugk, M.; Frauenheim, T.; Suhai, S.; Seifert, G. *Phys. Rev. B* **1998**, *58*, 7260.
(22) Brooks, C. L. III, Karplus, M. *J. Mol. Biol*. **1989**, *208*, 159.
(23) Simonson, T.; Archontis, G.; Karplus, M. *J. Phys. Chem. B* **1997**, *101*, 8349.
(24) Reuter, N.; Dejaegere, A.; Maigret, B.; Karplus, M. *J. Phys. Chem. A* **2000**, *104*, 1720.
(25) Brooks, B. R.; Bruccoleri, R. E.; Olafson, B. D.; States, D. J.; Swaminathan, S.; Karplus, M. *J. Comput. Chem*. **1983**, *4*, 187.
(26) (a) Bohr, H. G.; Jalkanen, K. J.; Elstner, M.; Frimand, K.; Suhai, S. *Chem. Phys*. **1999**, *246*, 13. (b) Elstner, M.; Jalkanen, K. J.; Knapp-Mohammady, M.; Frauenheim, T.; Suhai, S. *Chem. Phys*. **2000**, *256*, 15. (c) Elstner, M.; Jalkanen, K. J.; Knapp-Mohammady, M.; Frauenheim, T.; Suhai, S. *Chem. Phys.* **2001**, *263*, 203.
(27) Cui, Q.; Elstner, M.; Karplus, M. *J. Phys. Chem. B* **2002**, *106*, 2721.
(28) (a) Becke, A. D. *Phys. Rev. A* **1988**, *38*, 3098. (b) Lee, C.; Yang, W.; Parr, R. G. *Phys. Rev. B* **1988**, *37*, 785. (c) Becke, A. D. *J. Chem. Phys*. **1993**, *98*, 5648.
(29) (a) Ditchfield, R.; Hehre, W. J.; Pople, J. A. *J. Chem. Phys*. **1971**, *54*, 724. (b) Hehre, W. J.; Ditchfield, R.; Pople, J. A. *J. Chem. Phys*. **1972**, *56*, 2257. (c) Hariharan, P. C.; Pople, J. A. *Theor. Chim. Acta*. **1973**, *28*, 213.
(30) Torrie, G. M.; Valleau, J. P. *J. Chem. Phys*. **1977**, *23*, 187.
(31) Ryckaert, J. P.; Ciccotti, G.; Berendsen, H. J. C. *J. Comput. Phys*. **1977**, *23*, 327.
(32) Kumar, S.; Bouzida, D.; Swendsen, R. H.; Kollman, P. A.; Rosenberg, J. M. *J. Comput. Chem*. **1992**, *13*, 1011.
(33) The value was converted from the k_{cat} value (220 s^{-1}) cited in ref 9 with transition state theory, assuming a prefactor of kT/h, which was found to be appropriate in earlier studies (e.g., ref 16).
(34) Cui, Q.; Elstner, M.; Kaxiras, E.; Frauenheim, T.; Karplus, M. *J. Phys. Chem. B* **2001**, *105*, 569.

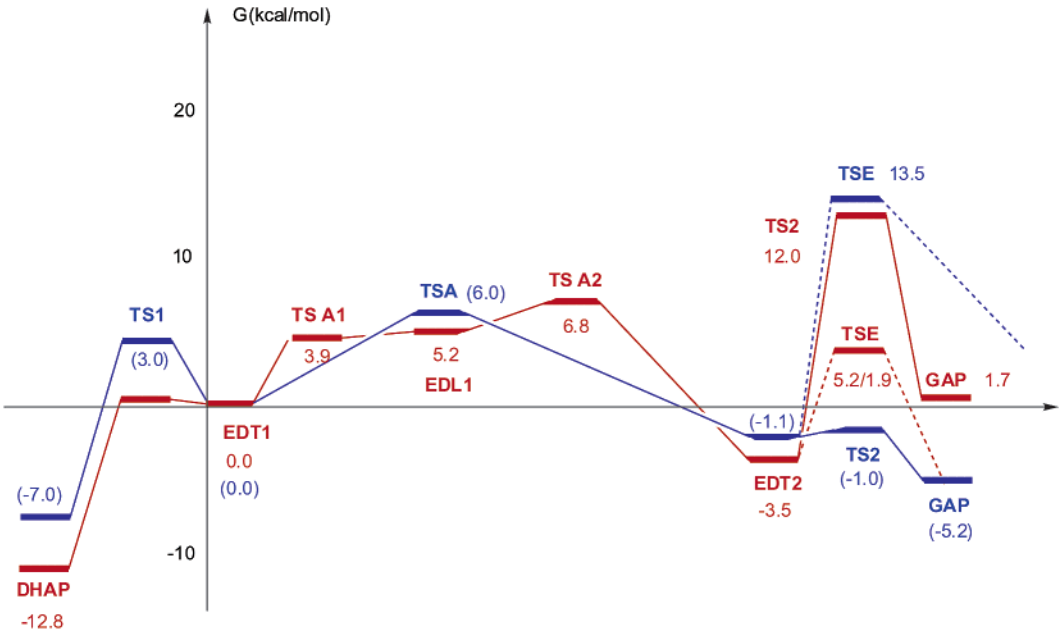

Figure 2. The schematic effective free energy surfaces (in kcal/mol) for the isomerization (solid line) and phosphate elimination reactions (dotted line) in MGS (in red) and TIM (in blue). The values without parentheses are from SCC-DFTB/CHARMM calculations in the current work, and these with parentheses are from previous study by one of the authors (ref 16), which were obtained at the B3LYP/6-31+G(d,p)/CHARMM level. The zero-point energies and vibrational free energy contributions were included with harmonic approximations based on SCC-DFTB/CHARMM normal-mode analyses for the critical structures. For the conversion between EDT1 and EDT2, which has several alternatives, the "classical" TIM-like mechanism (Scheme 1) was used here, because it was found to be energetically reasonable in both enzymes;[16,18] however, calculations found that other pathways are also likely to contribute in TIM[16] and MGS[18] with similar energetics. Note that wild type TIM catalyzes the interconversion of DHAP and GAP through TS2, while MGS catalyzes the conversion from DHAP to methylglyoxal, which involves phosphate elimination of EDT2 through TSE. The SCC-DFTB/CHARMM calculations correctly reproduced the functional specificity of the two enzymes. The values before and after the slash for TSE in MGS are the barriers without and with protonating the leaving phosphate group by Lys 23 (see text).

force calculations for MGS.[18] To account for vibrational effects (e.g., zero point motions) that can contribute significantly to the barrier heights in proton transfers, normal-mode analyses were carried out at critical points, and the vibrational contributions (zero point energy and vibrational entropy) were estimated with the harmonic approximation. Residues within 8 Å from the substrate were included in the vibrational calculations, and atoms beyond that were fixed (they were allowed to move in adiabatic mapping calculations). For the phosphate elimination, which might depend more sensitively on the protein environment, umbrella sampling simulations[30] were carried out in addition to reaction path optimizations to evaluate the consistency of the two approaches. The breaking C−O bond distance was taken as the approximate reaction coordinate, and 15 windows were chosen with the center of the umbrella potential ranging from 1.35 to 2.15 Å. Hybrid Langevian dynamics (LD) and molecular dynamics (MD) simulations associated with the stochastic boundary condition[22] used the umbrella sampling calculations; the LD/MD boundary was about 22 Å from the substrate, and was updated every 25 steps of integration. An integration time-step of 1 fs was used, with all the bonds involving hydrogen atoms constrained using SHAKE.[31] Each window was equilibrated for 20 ps, which was then followed by 20 ps of production simulation. Distributions of the C−O distances were then inverted to obtain the potential of mean force (PMF) for the phosphate elimination with the weighted histogram (WHAM) method.[32] The starting structure for the PMF simulation is the EDT2 intermediate, which came out of the calculations for the proton-transfer part of the reaction (Scheme 1).

For the reactions in TIM, the effective free energy profiles associated with the proton-transfer steps were taken from previous study at the B3LYP/6-31+G(d,p)/CHARMM level.[16] For the phosphate elimination, SCC-DFTB/MM simulations were carried out with a protocol similar to that used for MGS with the 7TIM structure;[7] the latter structure was also used in ref 16.

Finally, to investigate factors that influence the intrinsic energetics associated with the elimination reaction of enediolate species, gas-phase calculations were carried out for EDT2 with different $O^2-C^2-C^3-O^3$ torsional angles (Figure 4; see Figure 1 for labels of atoms) and protonation states. The calculations were mainly carried out at the SCC-DFTB level, and B3LYP[28]/6-31+G(d,p)[29] calculations were also carried out for selected configurations as validation of the SCC-DFTB approach (see Supporting Information). MD simulations were also carried out for EDT2·MGS and EDT2·TIM complexes to investigate the average values and fluctuations of the phosphoryl torsional angle in the two enzymes. After 50 ps of equilibration with hybrid MD/LD (see above), 150 ps production runs were carried out.

III. Results and Discussions

GAP Formation Is Unfavorable in MGS. On the basis of the schematic free energy profiles shown in Figure 2, the apparent activation free energy barrier in MGS (for the overall elimination reaction) is on the order of 20 kcal/mol, which is several kilocalories per mole higher than the experimental estimate of 14.4 kcal/mol.[33] This discrepancy can be partly attributed to the fact that SCC-DFTB/CHARMM was found to overestimate the stability of DHAP (relative to EDT1) compared to B3LYP/6-31+G(d,p)/CHARMM calculations.[34] The energetics associated with the critical structures (intermediates and transition states) are rather similar in MGS and TIM for all the proton transfer steps up to the second enediolate species (EDT2). The last isomerization step, which is a proton transfer from the protonated catalytic base (Glu 165 in TIM, Asp 71 in MGS) to the substrate and thus converts EDT2 to GAP, has dramatically different energetics in the two enzymes. While the barrier is vanishingly small in TIM, it is much higher in MGS and is close to 16 kcal/mol. Therefore, the result is consistent with the fact that GAP formation has not been observed in wild-type MGS. The GAP−enzyme complex is more than 10 kcal/

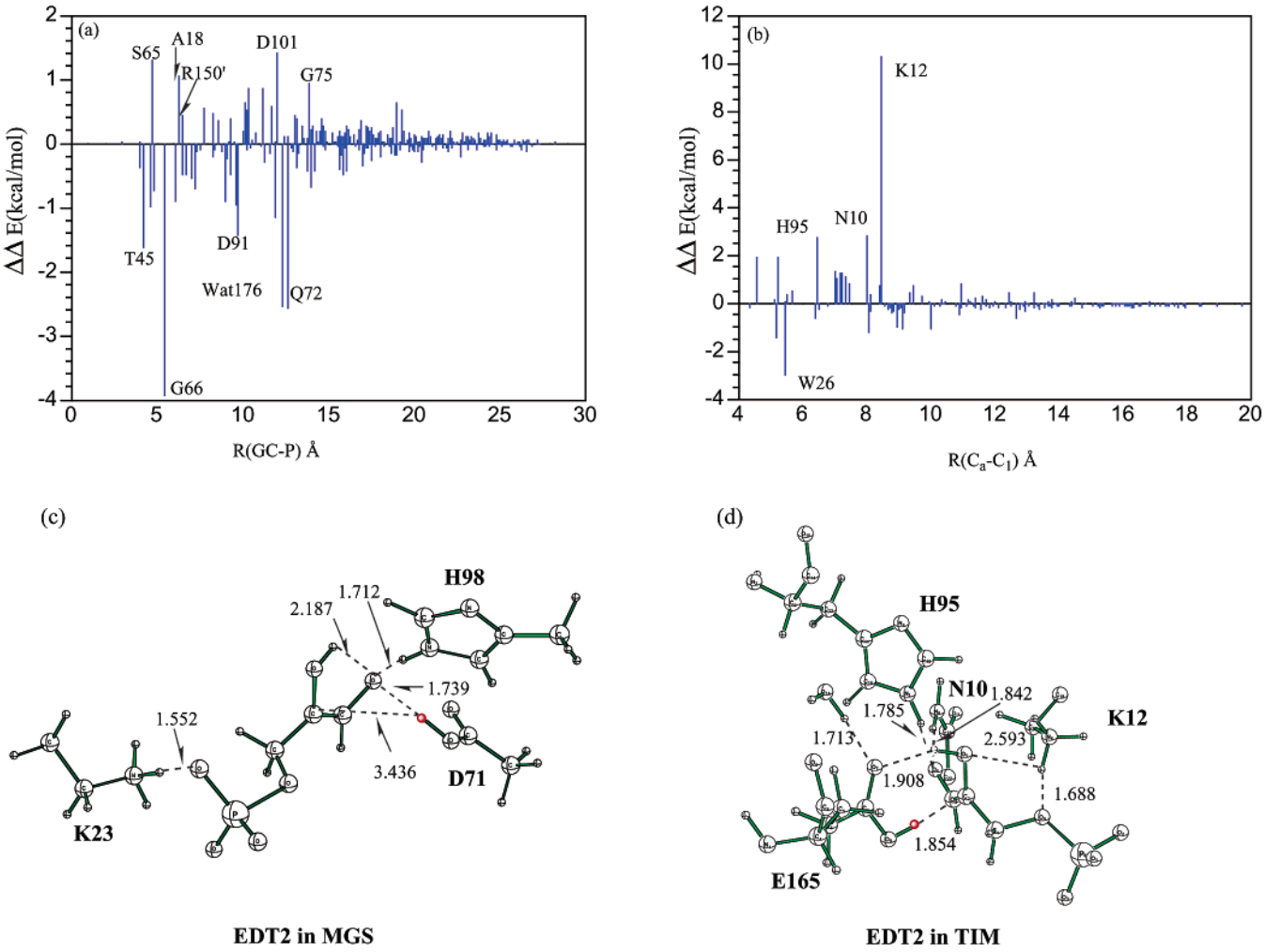

Figure 3. Results from perturbation analysis for the contributions from the protein residues and water molecules to the activation barrier of the EDT2 → GAP step in (a) MGS and (b) TIM. Results for TIM are from ref 16a, and results for MGS are from the current SCC-DFTB/CHARMM calculations. Negative values indicate favorable contributions that lower the activation barrier, while positive values indicate unfavorable contributions that increase the barrier. The *x*-axis indicates the distance between the residues and the substrate atoms. The active site structures with the substrate in the EDT2 state in (c) MGS and (d) TIM[16c] from QM/MM minimizations. Note that the distance (in Å) between the catalytic residue (Asp 71 in MGS and Glu 165 in TIM) and the proton acceptor (C^2 in the substrate) is very different in the two enzymes.

mol less stable than the DHAP−enzyme complex in MGS, while they are of similar energetics in TIM; the result is consistent with the observation that GAP is not an inhibitor for the activity of MGS toward DHAP elimination. Such an experimental observation is also consistent with the fact that the computed reverse barrier (GAP → TS2) is very high in MGS.

As shown in Figure 3a, a perturbation analysis[16,17] for the forward barrier did not reveal any residues with large destabilizing contributions in MGS. In TIM (Figure 3b), the lysine residue close to the substrate (K12) has a significantly unfavorable contribution to the barrier; this is because K12 favors EDT2, in which the substrate is more negatively charged. There is no such major unfavorable contribution in MGS, although there are also positively charged residues, such as K23 and R150′ from the neighboring subunit, close to the substrate. However, these residues are much more engaged in stabilizing the phosphate group of the substrate in MGS than in TIM; e.g., compare the positions of K23 in MGS and K12 in TIM, which are shown in parts c and d of Figure 3, respectively. Consequently, the influences from K23 and R150′ on the EDT2 → GAP transformation are fairly small in MGS; e.g., R150′ contributes only 1 kcal/mol to the barrier height (Figure 3a). Thus, the present calculations indicate that the high barrier for GAP formation in MGS is due primarily to the greater separation of the proton donor (carboxylate oxygen) and acceptor (C2 in EDT2), which is a result of the reduced flexibility of D71 in MGS relative to E165 in TIM. As shown in Figure 3b, the proton−acceptor distance in EDT2 is less than 1.9 Å in TIM, while it is about 3.4 Å in MGS. The interesting consequence is that the D71E mutant of MGS might be a reasonable isomerase that produces GAP, which is supported by calculations.[18] Preliminary experimental measurements, however, indicate that this mutant has a surprisingly low substrate affinity and activity. More computational and experimental studies are currently underway to better characterize this mutant.

Elimination Is Suppressed in TIM. For the phosphate elimination reaction, the QM/MM calculations also gave results that are consistent with the natural specificities of the two

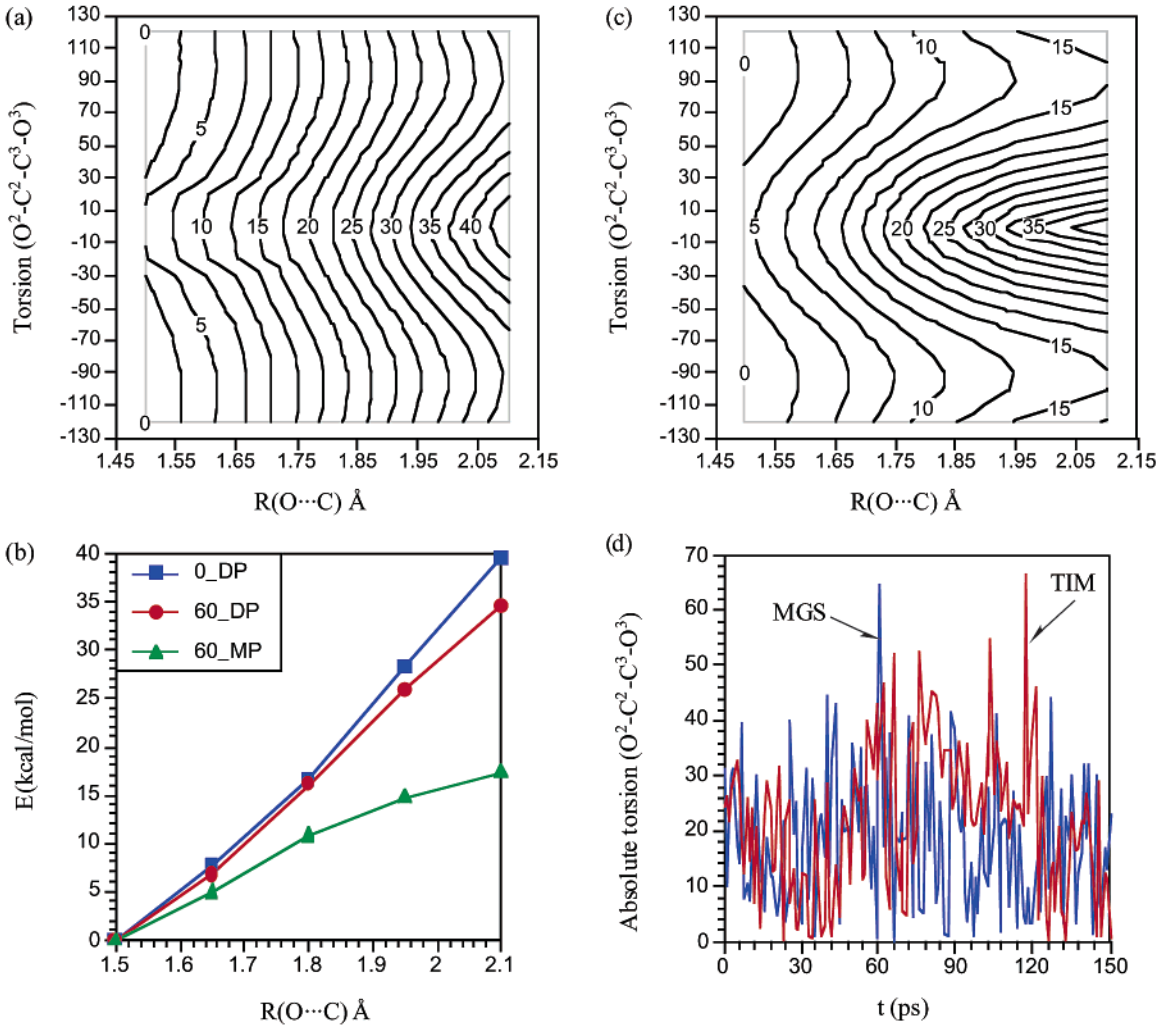

Figure 4. (a) The two-dimensional potential energy surface associated with the phosphate elimination from EDT2 in the gas phase; the two coordinates are the breaking C−O distance and the $O^2-C^2-C^3-O^3$ torsional angle. (b) The potential energy curve for the phosphate elimination as a function of the breaking C−O distance with different torsional angle or protonation state of the phosphate group (the torsional angle was fixed at all C−O distances). For the unprotonated phosphate case (DP), the torsional angles are close to these observed from X-ray structures for the two enzymes with PGH as the inhibitor, which was set to be 60° and 0° for MGS and TIM, respectively. In the protonated phosphate calculations (MP), the torsional angle was set to be 60°, because protonation appears only possible in MGS (see text). (c) Similar to part a, but with the phosphate group in EDT2 being monoprotonated. (d) The substrate $O^2-C^2-C^3-O^3$ torsional angles in MD simulations of MGS·EDT2 and TIM·EDT2. In parts a−c, which were done in the gas phase, SCC-DFTB was used. In part d, the MD simulations were made with the SCC-DFTB/CHARMM potential in a stochastic boundary setup (see Computational Method).

enzymes. The barrier in TIM is very large, on the order of 14 kcal/mol, which is consistent with previous experimental estimates for the fraction of elimination in TIM.[13] For MGS, the barrier is about 8.7 kcal/mol measured from EDT2. The popular explanation for such a difference in the two enzymes, which has been widely accepted, is the stereoelectronic hypothesis (see the Introduction).[4] It was argued that the $O^2-C^2-C^3-O^3$ torsional angle in the substrate has a large impact on the elimination activity, which was partially supported by the observation that the $O^2-C^2-C^3-O^3$ torsional angle is different in the X-ray structures of TIM and MGS with different inhibitors (it is ∼45° in MGS and ∼15° in TIM for PGH, and ∼55° in MGS and ∼5° in TIM for PGA). Our current theoretical analysis, however, does not directly support such a stereoelectronic effect being the dominant factor. As shown in Figure 4a, the torsional dependence of phosphate elimination in EDT2 in the gas phase is fairly small; e.g., with the torsional angle fixed at 60° (MGS like) and 0° (TIM like), the energy cost associated with the elimination reaction only differs by about 4 kcal/mol at the C−O distance of 2 Å (Figure 4b). When the phosphate is protonated, the torsional dependence becomes substantially more pronounced (Figure 4c), which is consistent with the notion that stabilizing the leaving phosphate group has a major influence on the effect of charge delocalization. In the active site of the enzyme, the leaving phosphate might be stabilized by nearby polar residues or water molecules (see below), and thus the torsional dependence is likely to be somewhere between the situations in Figure 4a,c. However, a major argument against the stereoelectronic hypothesis is the observation that the $O^2-C^2-C^3-O^3$ torsional angle is very similar in TIM and MGS with the EDT2 intermediate. Although this torsional angle was somewhat different in the X-ray structures of TIM and MGS with different *inhibitors*, the current MD simulations found very similar average torsional angles for the intermediate (EDT2) in the two enzymes; the average absolute $O^2-C^2-C^3-O^3$ torsion (Figure 4d) of TIM and MGS is 21° and 18°, respectively, with similar magnitude of fluctuations of 12°. In other words, even if the torsional dependence of phosphate elimination is larger than that found for EDT2 in the gas phase (Figure 4a,b), it is

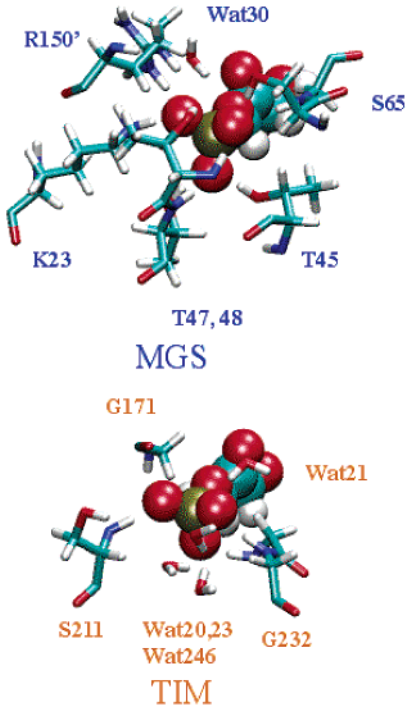

Figure 5. The environment of the substrate phosphate group in (a) MGS and (b) TIM, based on the relevant X-ray structures with PGH as the substrate inhibitor. Residues and water molecules within 3.5 Å of the substrate P atom are shown. Note that there are many more hydrogen bonding interactions between protein residues and the phosphate group in MGS than in TIM.

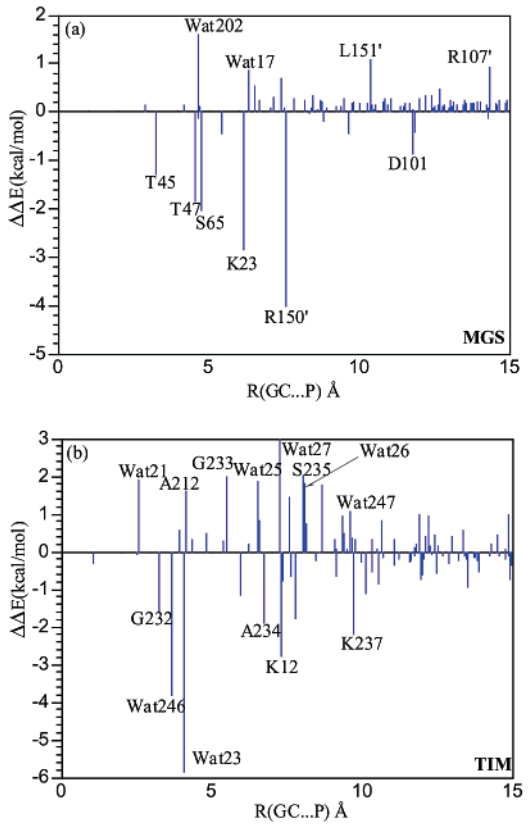

Figure 6. Results from perturbation analyses for the contributions (in kcal/mol) of protein residues and active-site water molecules to the elimination barrier in (a) MGS and (b) TIM. Although potential of mean force calculations were made, the perturbation analyses were more straightforwardly done with reaction paths for the elimination reaction. Negative (positive) values indicate stabilizing (destabilizing) contributions. The *x*-axis is the distance between the center-of-geometry of a particular group to the P atom in the substrate (in Å).

unlikely that the effect is the major origin for the catalytic specificities of TIM and MGS.

What could be the dominant factor that favors the elimination reaction in MGS than TIM? The current work supports the idea that the electrostatic environment of the leaving phosphate group plays an essential role. As noticed in previous work,[8,9] there are far more hydrogen-bonding interactions involving the substrate phosphate group in MGS (∼11) compared to TIM (∼2) (Figure 5). As shown in Figure 6, a perturbation analysis[17a] clearly illustrated that several polar and charged residues in MGS make substantial contributions to lower the elimination barrier; this includes Lys 23 (∼2.8 kcal/mol), Arg 150′ (∼4.0 kcal/mol), Ser 65 (∼2.1 kcal/mol), and Thr 45 and 47 (∼1.5 kcal/mol each). In TIM, only lysine residues (12 and 237) make sizable stabilizing contributions on the order of 2 kcal/mol. Active site water molecules were found to make substantial contributions in TIM, although their effects tend to cancel out and the net contribution is small.

Moreover, we note that another potential effect that might further lower the phosphate elimination barrier in MGS is a proton transfer from Lys 23 to the leaving phosphate group in EDT2. Solution measurements suggested that protonation of the phosphate makes it a better leaving group and increases the elimination rate by about 2 orders of magnitude;[12,13] gas-phase model calculations also suggest that protonation has a much more significant effect on elimination compared to the backbone torsional angle in EDT2; e.g., at the C−O distance of 2.0 Å (which is close to the value of the C−O distance in the transition state of phosphate elimination in both MGS and TIM), changing the $O^2-C^2-C^3-O^3$ torsional angle from 0° to 60° has an effect of 4 kcal/mol, while changing the protonation state of the phosphate has an effect more than 13 kcal/mol (Figure 4b). QM/MM calculations with both SCC-DFTB and AM1 as the QM method found that the barrier for the proton transfer from Lys 23 to the phosphate in EDT2 is vanishingly small (<2 kcal/mol) in MGS. Given that AM1 typically overestimates the barrier for proton transfers, it is unlikely that the low proton-transfer barrier found here is a calculation artifact. By contrast, the barrier is very high (>30 kcal/mol) in TIM due to the further separation between Lys 12 and the phosphate oxygen atoms (see Figure 3c,d). With the protonation of the phosphate, the elimination barrier in MGS becomes 5.5 kcal/mol; it is 3.2 kcal/mol lower than the unprotonated phosphate, which is comparable to the effect of protonation found in solution measurements.[12,13]

IV. Concluding Discussions

Enzymes are unique catalysts in that they are not only efficient but also highly specific.[1] Their catalytic specificity is reflected in terms of both selecting a particular substrate and carrying out specific chemical modifications with a small amount of side reactions. Therefore, understanding enzyme catalysis should stress both issues of reaction acceleration and side-reaction suppression.

In the current work, we applied combined QM/MM calculations to analyze the catalytic specificities of two enzymes: triosphosphate isomerase (TIM) and methylglyoxal synthase (MGS). With similar active site constructs, the two enzymes bind to the same substrate, dihydroxyacetone phosphate (DHAP),

but carry out different subsequent chemical modifications. While TIM catalyzes the isomerization of DHAP to glyceraldehyde phosphate (GAP),[10] MGS leads to the formation of methylglyoxal through a series of proton-transfer reactions and a phosphate elimination step.[9]

With an approximate density function theory (SCC-DFTB)[21,34] as the QM method, it is satisfying to see that the QM/MM calculations correctly reproduced the functional specificities of these two enzymes. In agreement with the previous proposal,[9] GAP formation is not favored in MGS; this is mainly due to the fact that the catalytic residue, Asp 71, is less flexible than Glu 165 in TIM. The further separation between the proton donor group (Asp 71) and acceptor atom (C^2 in EDT2) in MGS therefore requires a high activation barrier to carry out the proton transfer that leads to the formation of GAP. For the suppression of phosphate elimination in TIM, although it is still possible that the stereoelectronic effect associated with the phosphate torsional angle plays a role, the current theoretical analysis indicates that it is unlikely to be the dominant factor as previously believed.[4,9] First of all, the effect of the phosphoryl torsional angle on phosphate elimination in gas-phase EDT2 (unless protonated) is rather small at C−O distances around 2 Å, i.e., the region of the corresponding transition state in both MGS and TIM. Furthermore, MD simulations found very similar values for the average and fluctuation in the phosphate torsional angle in TIM·EDT2 and MGS·EDT2 complexes. The combination of these two findings led us to the conclusion that the "stereoelectronic" effect is not the dominant factor that controls catalytic specificities in MGS and TIM; indeed, stereoelectronic barriers can be easily circumvented in flexible systems. Thus, the current theoretical analysis supports the idea that it is the dissimilar electrostatic environment of (and possibly a proton transfer to) the phosphate group that leads to the significantly different energetics associated with the elimination process in the two enzymes.

The current study highlights the power of combining theoretical analysis with experimental techniques such as X-ray crystallography in understanding subtle issues in enzyme catalysis. This is because calculations are capable of providing a semiquantitative measure of the relative importance of factors that all seem physically reasonable. Combined with progress in the understanding of sequence dependence of protein structures, QM/MM approaches will be increasingly useful in the "rational" design of enzymes with defined catalytic efficiency and specificities.

Acknowledgment. The current research is supported by a start-up fund from the Department of Chemistry and College of Letters and Science at University of Wisconsin—Madison. Part of the calculations was done at the NCSA supercomputer center. Q.C and X.Z. thank Mr. A. Van Wynsberghe for critically reading the manuscript. D.H.T.H is grateful for the support from a NSF grant (MCB 0213347).

Supporting Information Available: A comparison between SCC-DFTB and B3LYP/6-31+G(d,p) calculations for the phosphate elimination reaction in a model complex in the gas phase is included to establish the reliability of SCC-DFTB for the reactions of interest in the current work.This material is available free of charge via the Internet at http://pubs.acs.org.

JA027063X